Progress Chinese Science Bulletin

High-Energy Physics January 2011 Vol.56 No.3: 238–244
doi: 10.1007/s11434-010-4289-7

Comprehensive test stand for high-intensity cyclotron development

ZHANG TianJue*, LI ZhenGuo, CHU ChengJie, XING JianSheng, GUAN FengPing, ZHONG JunQing, JI Bin, GE Tao, YIN ZhiGuo, HOU ShiGang, PAN GaoFeng, YAO HongJuan, LU YinLong, WANG ZhenHui, WU LongCheng, LIN Jun, JIA XianLu, WEI SuMin, WEN LiPeng, WANG Feng, XIA Le, CAI HongRu, XIE HuaiDong, CHEN RongFan, ZHANG Yan, ZHANG SuPing, LIU GengShou, ZOU Jian, AN ShiZhong, YANG JianJun, BI YuanJie & YANG Fang

China Institute of Atomic Energy, Beijing 102413, China

Received September 5, 2010; accepted October 28, 2010

A comprehensive test stand for high-intensity cyclotron development, a 10 MeV 430 μA cyclotron, has been successfully constructed at China Institute of Atomic Energy (CIAE) for the experimental verification of the viability of a 100 MeV high-intensity cyclotron (CYCIAE-100) being constructed at CIAE. The verification includes the overall design technology, detail design and engineering technology for the crucial parts of the machine, e.g. main magnet and beam diagnostics. It will also pave the way for future enhancement of the beam intensity. The test stand consists of a H^- ion source, axial injection system, central region, main magnet and coil, RF resonator, stripping extraction, and auxiliary systems, which include the RF power amplifier, high voltage and DC power supplies, electric apparatus, beam diagnostics, control, vacuum, water cooling, pneumatic system, and safety interlock. This paper presents the work regarding the design and sub-system development of the test sand, and the results of the beam commissioning of the machine.

cyclotron, main magnet, RF system, beam diagnostics

Citation: Zhang T J, Li Z G, Chu C J, et al. Comprehensive test stand for high-intensity cyclotron development. Chinese Sci Bull, 2011, 56: 238–244, doi: 10.1007/s11434-010-4289-7

In addition to the applications in homeland security, high-intensity proton beams have applications in fundamental research on nuclear physics and material and life sciences, applied research in nuclear energy, industrial and agricultural production, and medical science [1–3]. The wide applications promote the research in the key area of high-intensity cyclotrons in China [4]. Studies on accelerator physics and engineering technology from the H^- beam production, injection, acceleration, and stripping extraction have been conducted at China Institute of Atomic Energy (CIAE) since 2001. This includes some frontier issues concerning high intensity cyclotron study, e.g. strong focusing straight sector magnets, high stability RF system, high efficiency injection, extraction system, beam dynamics and beam losses. After the individual experimental systems were accomplished in sequence, they were integrated into the comprehensive test stand for high-intensity cyclotron study, known as CYCIAE-CRM. The test stand serves as a high-intensity-cyclotron experimental research platform to test some of the critical technologies for the planned CYCIAE-100. This installation can be used for the future goal of developing a MW high-intensity cyclotron at the mA level. It is also the first compact cyclotron made in China that has proprietary intellectual property rights, capable of accelerating H^- ions to 10 MeV, and extracting protons through stripping. In this sense, it has laid a solid foundation for the industrialization and commercialization of PET cyclotrons. The main technical parameters are

*Corresponding author (email: tjzhang@ciae.ac.cn)

shown in Table 1.

1 Development of the 10-mAH-multicusp ion source

To achieve high plasma density in the multicusp ion source, a specially shaped filament made of Ta-alloy was selected based on the results of hundreds of experiments and many material and shape comparisons. The permanent magnets of alternate polarity were placed around the discharge chamber. An azimuthal magnet was placed between every two alternate magnets to create a strong multicusp magnetic field for plasma confinement. The traditional method of electron filtering, i.e. inserting water cooled dipole columns in the chamber, was replaced. In this case, the top azimuth magnet was removed and the polarities of a pair of radial magnets in the center line were changed from "N" to "S". Two pairs of permanent magnets with a cross sectional size of 3 mm×5 mm were embedded in the extractor of the three-electrode extraction system. This design can increase the ability of the filter magnetic field to filter electrons and can correct the direction of extracted H^- ions.

By increasing multicusp magnetic field and developing the virtual-filter magnetic field, the amount of H^- ions in the chamber and extracted beam density are increased, with the average beam intensity increased to 10 mA. The ion source test stand is shown in Figure 1(a), and after numerous tests, it was found that the H^- beam is stable, at intensities higher than 10 mA during long term operation. The beam profiles are shown in Figure 1(b) The full-width-at-half-maximum diameter is only 5–7 mm.

2 Design and construction of injection line and central region

(i) The injection line. To match the acceptance of the spiral inflector in the central region, a specially designed solenoid and doublet were adopted as the transverse focus elements on the injection line. The influence on the injected beam envelope from different neutralization rates was studied. In order to fit the calculation of optics matching, the code TRANSOPTR has been improved, in which the beam optics method of spiral electrostatic inflector in high flutter field, stray field in central plug of the main magnet and the setting of matching goal for the circulating beam in first turn, has been innovatively developed. In this way, the injection efficiency can be effectively improved through accurate numerical simulation of the complex injection process. The layout and a picture of the axial injection line are shown in Figure 2.

(ii) The design of spiral inflector and central region. Under the effect of the magnetic field in the central region, the vertical injection beam is injected spirally into the midplane of the machine. In this process, the electric field in the

Table 1 Main technical parameters of CYCIAE-CRM

Beam			Ion Source	
Accelerated ions	Beam intensity		Type	Arc power
	internal target	extracted		
H^-, 10 MeV	H^-, 430 μA	proton, 230 μA	H^- multicusp	2.5 kW
Magnet structure				Beam extraction
No. of sectors	Sector angle	Peak field	Coil power	
4	50°–54°	1.75 T	6 kW	stripping extraction
RF system				Control
RF power	No., angle of Dee	Frequency	D voltage	
13.5 kW	2, 30°	70.5 MHz	40 kV	PLC based auto control

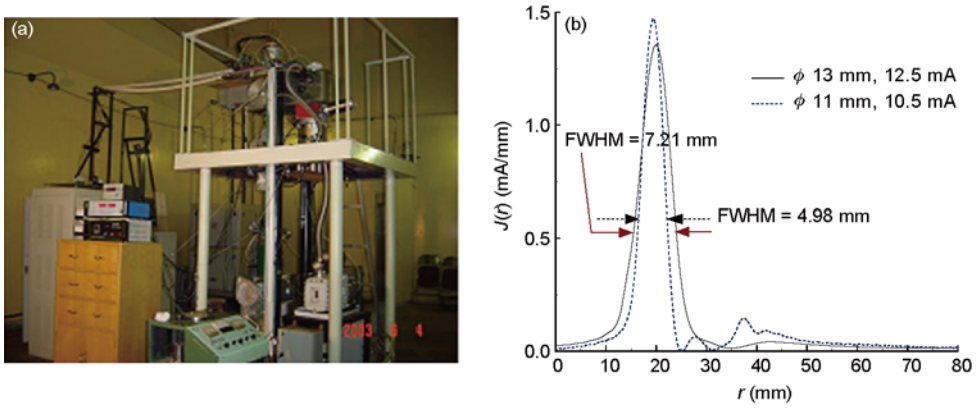

Figure 1 A picture of the test stand for H^- ion source (a) and a cross section of the extracted beam (b).

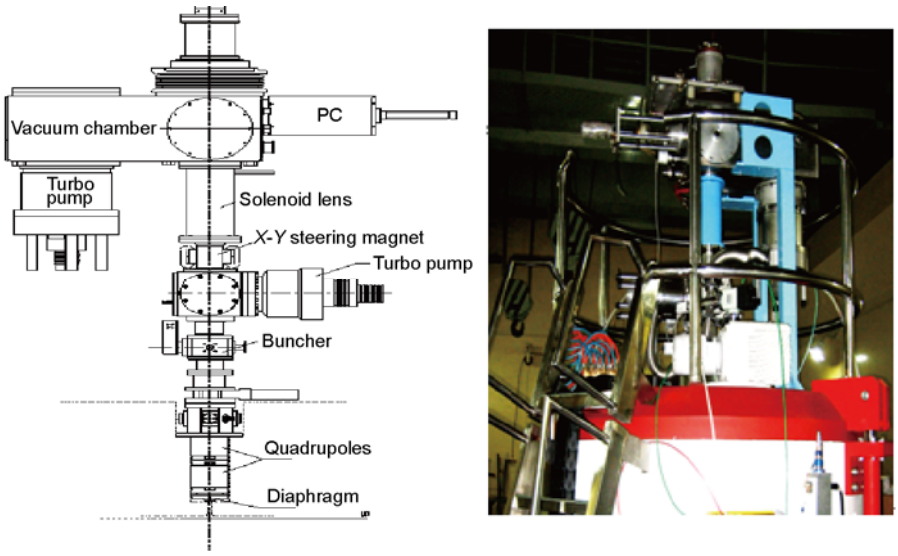

Figure 2 Layout and picture of the axial injection line.

inflector always stays perpendicular to the trajectory of the central particle, which keeps the injection energy constant. Table 2 shows the parameters of CYCIAE-CRM inflector.

While designing the central region, we took the lead in studying automatic transfer techniques from AUTOCAD drawing to the electrode discrete grid for *E*-field simulation. In-depth research had been carried out on the beam dynamics of multi-field coupling in the narrow central region, e.g. the RF field formed by the complex electrode boundary, high voltage electric field of the spiral static inflector, and the large flutter static, magnetic field. It had been realized that the RF acceptance is as high as 40°. Figure 3 shows the trajectory tracking results which indicate that the beam is well centered, and a photograph of the inflector and the central region.

(iii) Machining and installation of the inflector and the central region. Based on the central trajectory of the inflector, the four edge curves form the spiral electrode and the height of the electrode. A special program was developed to take designs from fundamental physics to create command for NC machining, which has overcome the difficulty in machining the spiral electrostatic inflector. The electrode in the central region was also fabricated by the NC machining center. Because the parallelism of the upper/lower flanges is less than 0.01 mm, the flanges were polished by abrade. The gap between ground electrode and the Dee tip has strict requirements, and during installation, a special "go-no-go gauge" for the electrode gap was made to control the precision of the electrode gap to within ±0.05 mm [5].

3 Beam loss study

Because the binding energy of the outermost electron in H^- ion is only 0.755 eV, there are many types of beam loss in the H^- cyclotron. The two major causes of beam loss can be attributed to the Lorenz force and vacuum dissociation by residual gas.

During the cyclotron operation, the portion of beam that is lost will hit the vacuum chamber or the RF cavity, and will emit neutrons and γ-radiation, producing high radiation doses. In the cyclotron, the radiation consists of two parts, one is the radiation incident on the vacuum chamber directly from lost beam, and the other portion is produced by cascaded neutron inside the chamber wall, which results in radionuclides being trapped in the chamber walls and consequently generating residual doses. The results of beam loss study and M-C simulations will place strict technical requirements on the vacuum system, and determine the op-

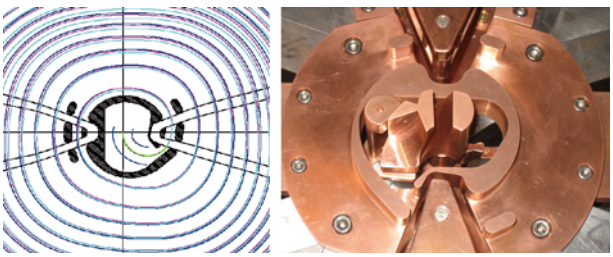

Figure 3 Beam trajectory with a phase width of 40° and a photograph of inflector and central region.

Table 2 Parameters of the CYCIAE-CRM inflector

Injection energy	Electrode height	Electric bending radius	Slope factor	Electrode gap	Electrode width	Bending angle at entrance	Voltage
30 keV	31 mm	32.06 mm	0	8 mm	16 mm	260°	±7.46 kV

timal materials for the chamber to reduce the residual radiation.

4 Main magnet

The main magnet possesses the following features: it has a compact structure with four sectors; it uses a straight-edge pole shape, which not only meets the requirements of accelerator physics, but also enables convenient machining and installation of poles and RF cavities; the gap between sectors varies with radius, which will decrease the required angle of the poles at the outer radius and will obtain high vertical focusing for the high intensity beam; the cyclotron design uses a deep valley, which will increase the flutter of the magnetic field and further enhance the vertical focusing.

(i) Physical design. The final energy was determined by the magnetic rigidity. The peak field in the median plane was set at 1.75 T, and the angle of the sectors was 52°. Therefore, the 10 MeV beam will be extracted at a radius of 41 cm. The radius of the poles and hill gap are 45 cm and 2.3 cm, respectively. Through numerical study and beam dynamics analysis, we realized the fringe-field shimming with a straight edge sector magnet. Therefore, the vertical focusing was effectively enhanced. By adjusting the parameters of the magnet, the phase shift is controlled within ±10°, and the vertical oscillation frequency is higher than 0.5. In addition, the Walkinshaw resonance is avoided at the large radius. Based on the theoretical calculations and studies of the high-intensity-beam dynamics under the calculated field, the beam dynamics, such as the accelerated beam orbit and beam emittance, were determined. The machining and assembly tolerance for the magnet was determined through the studies of effects induced various factors, e.g. the first harmonic and field B_r.

(ii) Mechanical design and construction. As the key part of the construction of the CYCIAE-CRM, the fabrication of the main magnet requires high-precision processing. The difficulties in dealing with the mechanical design and machining were primarily concerned with ensuring that the four pairs of poles had the same angle, symmetric assembly, and precision control of the hill gap between sectors. Therefore, before the magnet was processed, a set of exclusive pattern plates was designed and fabricated that fully met the angle and symmetry requirements. With the pattern plate, the machining precision of the pole angle was better than 0.003°. A set of tools was specially designed for the assembly of the straight poles in the deep valley, which solved the technical problems related to high-precision pole installation. A special material milling cutter was designed and fabricated. Once implemented, the milling cutter processed the surface of the eight sectors without exceeding the abrasion tolerance. Those methods effectively ensured that deviation of the gap was less than 0.02 mm. The final installation and assembly of the magnet was accomplished with strict quality control processes to satisfy the demands of the design.

(iii) Mapping and shimming of the magnetic field. Polar coordinates were used in the magnetic-field measurements. A method using separate positioning and driving systems was adopted in the design of the mapper. In the azimuthal direction, the angle position of the Hall probe was controlled by an angle encoder and servo system. In the radial direction, the radial position of the probe was controlled by the high-precision measurement blocks. For vertical positioning, a support module was used to adjust the height of the rotating arm. After the mapper was installed, the measurement accuracy in the radial position was 0.1 mm, and the angular accuracy in azimuthal direction was 5″.

The shimming method for isochronous fields was independently developed at CIAE, and is based on the NC machining of the continuous profile of the shimming bars, through which high-precision field shimming can be achieved. Meanwhile the method will reduce the shimming time. The improvement of the phase shift and axial focusing, which results from the high-precision mapping and shimming, is shown in Figures 4 and 5, respectively.

To obtain high-intensity beams and good beam quality, requirements have been put on the magnetic mapping and shimming based on the results of the numerical analysis of the bunches through beam dynamics. The first harmonic in the central and extraction region should be less than 15 G, which corresponds to less than 5 G in the acceleration region. Through numerical studies of the magnetic field, a new shimming method was developed using non-symmetric shimming-bar processing and high-precision NC machining at the profiles of shimming bars to reduce the non-ideal harmonic field. The method effectively reduces the first harmonic at all radii, and ensures the isochronicity of the magnetic field. The effect of the shimming process on the first harmonic is shown in Figure 6. The shimming-method effect on the harmonic field effectively reduces the technical requirements on internal steel defects, providing an experimental basis to address the technical issues related to

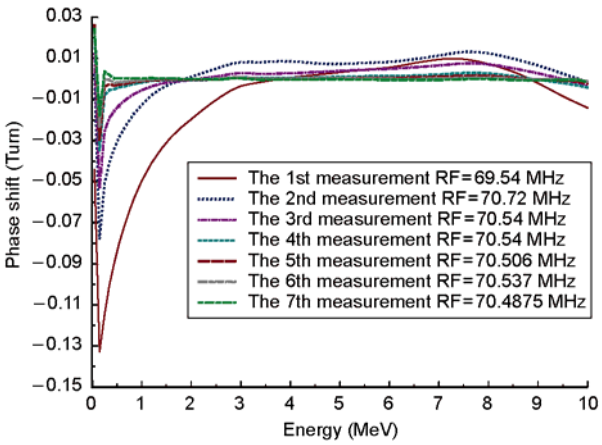

Figure 4 Phase shift change.

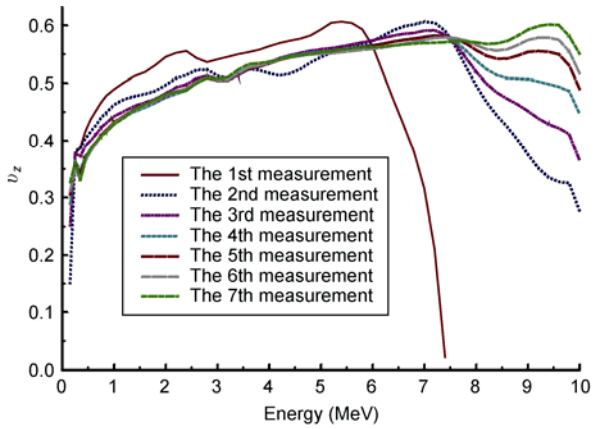

Figure 5 Axial focusing change.

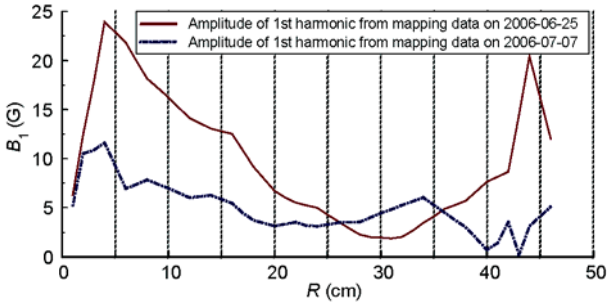

Figure 6 Effect of shimming process on the first harmonic.

casting steel in large-scale cyclotron magnet fabrication.

5 RF system

A set of RF resonators was specially designed to fit in the limited space of the valley in the compact cyclotron, while maintaining the quality factor to the greatest extent possible. With consideration for the high-Q load, transmission line and the ground-cathode final-stage used in this system, an equivalent circuit (transmission line model) for the high power RF section is obtained using key parameters. The parameters were identified from studies of the harmful parasitic resonance found in the conditioning, which was hunted down using the model and finally solved by neutralization. The optimization of the RF system of the CRM cyclotron continued for about two years, and the modifications were focused on low level circuits, high-power RF circuits, and the resonator. The result is briefly discussed below.

(i) RF power amplifier. The ground cathode amplifier, which was operated in Class AB, yields a high gain, acceptable efficiency, and good linearity. The tuning range for the amplifier is 69–72 MHz, with respect to the short plate position in the anode circuits. After switching to a transformer, with a higher anode potential, the output power at the fundamental frequency was increased from 9.8 kW to 13.9 kW.

(ii) Low level controls. The tuning circuits compare the phase difference between the cavity-feedback signal and the forward-power-pickup signal, and the error signal is then proportionally amplified to control the motion of the tuning capacitor. Thus, the resonance is kept equal to the driving frequency. The amplitude loop compares the feedback Dee voltage with the set-point voltage to generate an error signal, and a proportional-integral controller is used to amplify it. The amplified signal is used control an attenuator in the signal path between the source and amplifier chain.

(iii) RF buncher. A buncher is included in the injection line to increase the efficiency. To have a better phase stability in the cavity, a set of low level circuits was specially developed with feedback control for stability, to allow the buncher-driving signal to come from either the signal source or from the cavity pickup. The efficiency of the buncher was reported to be 2.4 in low beam intensity conditions.

(iv) The resonator. The major challenge of the cavity design is the limited space available in the compact cyclotron. Combining this requirement with other conventional high power design issues, e.g. mechanical and thermal stability, the system must be designed with a coaxial extension of the cavity, which is shown in Figure 7, to take space of the hole in the return yoke. The design began with the numerical 3D finite difference method (Figure 7), followed by with 1:1 scale wooden model prototyping, which confirmed the resonance frequency to be within 3% of the calculated value. Then the actual cavity was fabricated with a measured quality factor of 3682. In addition, the measured voltage distribution agreed with the simulation, as shown in Figure 8.

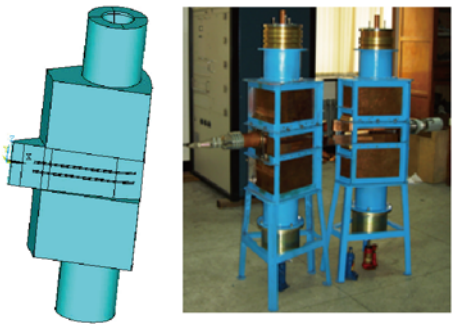

Figure 7 Resonator and its simulation model.

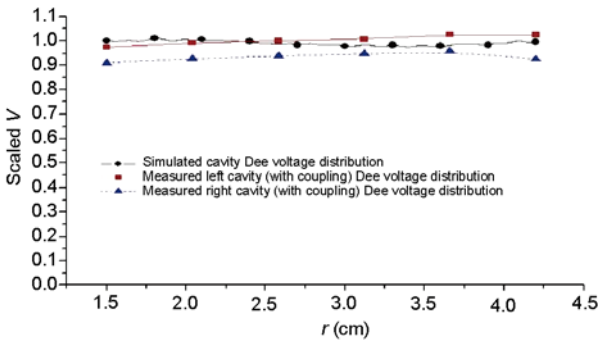

Figure 8 Dee-voltage distribution.

6 Vacuum

The vacuum system design concerns several parts, including the ion source, injection line and main chamber. A static vacuum of 1×10^{-6} mbar was required according to beam-loss simulation. High-purity hydrogen was vented into the ion source chamber (6 cm^3/min) during operation, and the dynamic pressures in ion source chamber, injection line, and main chamber were 3×10^{-5} mbar, 1×10^{-5} mbar and 2×10^{-6} mbar, respectively.

For the main vacuum system, oil contamination and H^--beam losses were greatly reduced after adopting polyphenylene ether (PPE) to replace the normal diffusion pump fluid. The use of Viton O-rings reduced the effect of radiation and prolonged O-ring lifetimes in the high-current environment, when compared with the use of normal O-rings. All the components in the cyclotron are nickel-plated and polished, to reduce surface outgassing.

According to the outgassing rate of the components, leakage, and vented hydrogen, a Turbo Molecular Pump (TMP) with a pumping speed of 1500 L/s was selected for the ion source, and a TMP with a pumping speed of 600 L/s was selected for the injection line. For the main chamber, two diffusion pumps with pumping speeds of 2400 L/s were used. A differential pump system was designed to reduce the introduction of hydrogen from the ion source into the main chamber.

7 Extraction system

Extraction via stripping foil has the advantages of high extraction efficiency and low current loss. Two sets of stripping systems are symmetrically placed at 180° in azimuth direction to achieve dual extraction, which greatly improves the extraction efficiency.

The stripping foil was inserted vertically into the machine to enable self-shielding. The extraction system is compact in structure and easy to control. The three foils can be changed automatically, which was realized via stepper motor and feedback through an angle encoder. The signal from this high-precision encoder was used to obtain the angle of the stripping foil, which controls the beam extraction direction.

By analyzing the relation of extraction efficiency with energy dissipation and life-span, a stripping foil with a surface density of 20 μg/cm^2 was selected. The measured efficiency was 99.87%, which agreed well with the calculated efficiency of 99.97%.

8 Beam diagnostics

The beam diagnostic system consists of three parts: the injection line, cyclotron interior and the beam line.

(i) Beam diagnostic device on the injection line. Faraday cup: A specially designed Faraday cup was used to control the beam profile, the beam emittance and the beam intensity. The basic structure is a slot in front of a square cylinder, and the current signal is amplified by an *I-V* converter. A perpetual magnet was used to restrain secondary electron emission, which enhanced the measurement precision of the H^- current.

DC current transformer: This system was tested with a range of DC currents, and the sensitivity was found to be 0.4%. The DC current transformer system can measure the beam intensity in real-time and in-line.

Double wire scanner and emittance scanner: The double wire scanner was used to measure the high-energy high-intensity beam. Two wires of high-temperature resistance material were crossed at a 90° angle and isolated from each other. The signal from the two wires was acquired separately. An improvement was made to the emittance scanner by adopting a multi-slot single wire to measure the emittance, which satisfies the specific demands of the high-intensity H^- current.

(ii) Beam diagnostics inside the cyclotron. A radial probe is used to measure the beam distribution inside the cyclotron. There are five isolated fingers. The position of the radial probe is controlled by a stepper motor and a feedback potentiometer with an accuracy of 0.1 mm. The structure of radial probe is shown in Figure 9.

The phase probe comprises several pairs of separated capacitor plates, which are symmetric about the mid-plane and distributed equally in radial direction. This is shown in Figure 10. By analyzing the signal phase with the phase probe, the error between the ideal isochronous field and the practical field in the radial direction can be obtained.

(iii) Beam monitoring in the extraction region. The power transferred from the Faraday cup to the beam line is

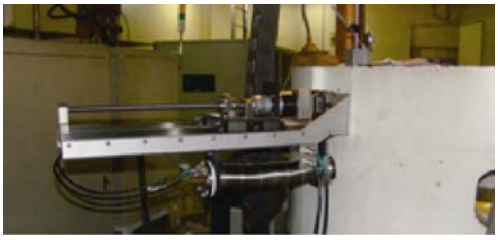

Figure 9 Structure of the radial probe.

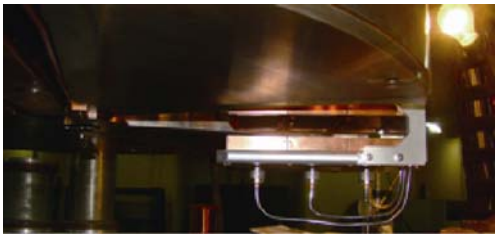

Figure 10 Experimental phase probe.

5 kW. Therefore, water cooling must be used. The head of the Faraday cup is shown in Figure 11. The taper structure increases the contact area with the beam to avoid high local power densities.

9 Controls

The design goal for the control system was to provide both an automated system and a remotely operable interface. In addition, the features such as ease-to-use, optimized process control and high stability were emphasized in the design procedures.

As a requirement of automatic operation, the main magnet system, the RF system and the extraction system are designed to have feedback regulations to minimize the beam loss to achieve high stability during high-intensity operation. From a safety perspective, the control system can stop the beam within micro seconds using one of many methods, including the cut-off of the RF acceleration voltage, disabling the HV output to the inflector, and injection of the Faraday cup of the ion source.

The control system uses a programmable logic controller to implement the device interlocks and monitor the cyclotron devices. The controller is also connected through a field bus to computer, in which the sophisticated logic and control strategy are carried out. The programmable logic controller is a robust executer, programmed using the STL language, and can operate without a computer. The field bus functions can be used for future upgrades of the control system.

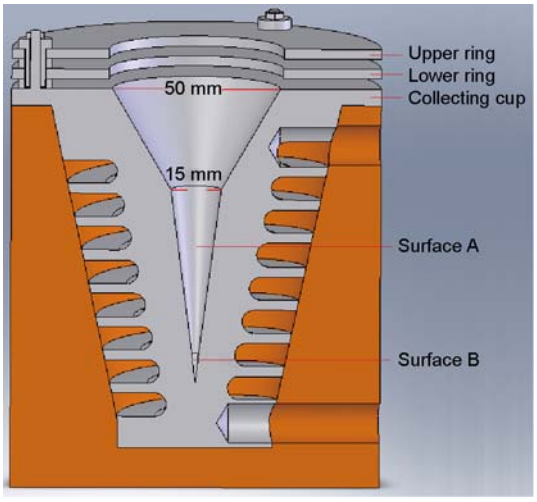

Figure 11 Head of the Faraday cup.

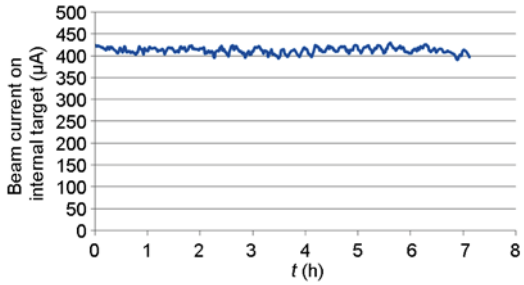

Figure 12 Beam intensity on the internal target during long-term operation.

10 Beam commissioning results

The beam commissioning of CYCIAE-CRM has been performed over nearly a 3-year time span. The beam intensity on the internal target has been as high as 430 μA and the stability is better than 0.5% over 8 h operation, which is shown in Figure 12. The overall efficiency, which includes the transport efficiency of the injection line, injection efficiency of the spiral inflector, and capture and acceleration efficiency of the RF phase, has reached 17.7%. With a 64% RF-system duty factor and an extracted beam intensity of 2.30 mA from the ion source, the beam intensity on the stripping target is 231.14 μA, which corresponds to 230.85 μA of the extracted beam. The extraction efficiency can be up to 99.87%, and the acceleration efficiency from the central region to the extraction region is approximately 94.5%.

This work was supported by the National Natural Science Foundation of China (10775185, 10805080).

1 Cooper N G. LANSCE into the Future. LA-UR-06-0515, LANL, 2006
2 Seidel M. Production of a 1.3 MW proton beam at PSI. In: Proceedings of 1st International Particle Accelerator Conference, Kyoto, 2010, TUYRA03
3 Kubota K. From tumor biology to clinical PET: A review of positron emission tomography (PET) in oncology. Ann Nucl Med, 2001, 15: 471–486
4 Zhang T J, Fan M W, Li Z G, et al. Research progress in high intensity cyclotron technology. Chinese Sci Bull, 2009, 54: 3931–3939
5 Yao H J. Theoretical and experimental study on axial injection and central region of cyclotron CYCIAE-100 (in Chinese). Ph. D. Thesis. Beijing: Tsinghua University, 2008